The G Protein β-Subunit, AGB1, Interacts with FERONIA in RALF1-Regulated Stomatal Movement[1][OPEN]

Yunqing Yu,[2] David Chakravorty, and Sarah M. Assmann[3]

Biology Department, Pennsylvania State University, University Park, Pennsylvania 16802

ORCID IDs: 0000-0003-2447-6161 (Y.Y.); 0000-0002-6591-4853 (D.C.); 0000-0003-4541-1594 (S.M.A.).

Heterotrimeric guanine nucleotide-binding (G) proteins are composed of Gα, Gβ, and Gγ subunits and function as molecular switches in signal transduction. In Arabidopsis (*Arabidopsis thaliana*), there are one canonical Gα (GPA1), three extra-large Gα (XLG1, XLG2, and XLG3), one Gβ (AGB1), and three Gγ (AGG1, AGG2, and AGG3) subunits. To elucidate AGB1 molecular signaling, we performed immunoprecipitation using plasma membrane-enriched proteins followed by mass spectrometry to identify the protein interactors of AGB1. After eliminating proteins present in the control immunoprecipitation, commonly identified contaminants, and organellar proteins, a total of 103 candidate AGB1-associated proteins were confidently identified. We identified all of the G protein subunits except XLG1, receptor-like kinases, Ca^{2+} signaling-related proteins, and 14-3-3-like proteins, all of which may couple with or modulate G protein signaling. We confirmed physical interaction between AGB1 and the receptor-like kinase FERONIA (FER) using bimolecular fluorescence complementation. The Rapid Alkalinization Factor (RALF) family of polypeptides have been shown to be ligands of FER. In this study, we demonstrate that RALF1 regulates stomatal apertures and does so in a G protein-dependent manner, inhibiting stomatal opening and promoting stomatal closure in Columbia but not in *agb1* mutants. We further show that AGGs and XLGs, but not GPA1, participate in RALF1-mediated stomatal signaling. Our results suggest that FER acts as a G protein-coupled receptor for plant heterotrimeric G proteins.

Heterotrimeric guanine nucleotide-binding (G) proteins are composed of Gα, Gβ, and Gγ subunits and function as molecular switches in signal transduction. The human genome encodes 16 Gα, five Gβ, and 12 Gγ genes (Jones and Assmann, 2004). However, the Arabidopsis (*Arabidopsis thaliana*) genome encodes only one canonical Gα (GPA1; Ma et al., 1990), three extra-large Gα (XLG1, XLG2, and XLG3; Lee and Assmann, 1999; Ding et al., 2008; Chakravorty et al., 2015), one Gβ (AGB1; Weiss et al., 1994), two canonical Gγ (AGG1 and AGG2), and one noncanonical Gγ (AGG3) subunits (Mason and Botella, 2000, 2001; Chakravorty et al., 2011).

Despite the limited numbers of G protein subunits in Arabidopsis, G proteins have been shown to participate in numerous processes related to plant development and organ morphogenesis (Perfus-Barbeoch et al., 2004;

Chakravorty et al., 2011; Urano et al., 2016b), cell wall composition (Delgado-Cerezo et al., 2012), hormone responses (Ullah et al., 2001, 2002, 2003; Wang et al., 2001; Pandey et al., 2006; Ding et al., 2008), responses to light stimuli (Warpeha et al., 2006; Botto et al., 2009), and biotic (Llorente et al., 2005; Zhu et al., 2009) and abiotic (Joo et al., 2005; Yu and Assmann, 2015; Urano et al., 2016a) stresses. In particular, both GPA1 and AGB1 play positive roles in aspects of abscisic acid (ABA)-mediated regulation of stomatal apertures. Both *gpa1* and *agb1* mutants are hyposensitive to ABA inhibition of stomatal opening but show wild-type responses to ABA promotion of stomatal closure (Wang et al., 2001; Fan et al., 2008). In the presence of a cytosolic pH clamp imposed with butyrate, *gpa1* also shows hyposensitivity to ABA-induced stomatal closure, suggesting a bifurcating stomatal closure network with GPA1-dependent and pH-dependent paths (Wang et al., 2001). Mutant analysis also has shown roles for GPA1 in ABA regulation of the guard cell transcriptome (Pandey et al., 2010) and metabolome (Jin et al., 2013).

Diverse roles of G protein signaling imply a diversity of upstream and downstream interacting partners. Components of the G protein interactome have been identified through yeast-two hybrid (Y2H) screens, including PIRIN1 (Lapik and Kaufman, 2003) and THYLAKOID FORMATION1 (Huang et al., 2006) as GPA1 interactors, Plant U-Box (PUB) E3 ubiquitin ligases, PUB2 and PUB4, as XLG interactors (Wang et al., 2017), and an auxin transport modulator, N-MYC DOWNREGULATED-LIKE1, as an AGB1/AGG2 interactor (Mudgil et al., 2009). Although current

knowledge indicates that Gβ and Gγ operate as an inseparable dimer, some Y2H screens used AGB1 alone and identified interactors such as PUB20 (Kobayashi et al., 2012), the 2C-type protein phosphatase PP2C52 (Tsugama et al., 2012), adaptor protein AP-3μ (Kansup et al., 2013), the bZIP transcription factor VIRE2-INTERACTING PROTEIN1 (Tsugama et al., 2013), NON-PHOTOTROPIC HYPOCOTYL3 (Kansup et al., 2014), and MAPK6 (MPK6; Xu et al., 2015). Similarly, by Y2H library screening with GPA1, AGB1, and several previously identified G protein interactors as baits, a large-scale G protein interactome was generated, within which an overrepresentation of proteins related to cell wall composition was identified (Klopffleisch et al., 2011). Of the above interactors, 2C-type protein phosphatases (Joshi-Saha et al., 2011) and MPK6 (Montillet et al., 2013; Li et al., 2017) have been implicated previously in stomatal aperture regulation.

Despite the fruitful progress in the identification of the G protein interactome from Y2/3H screening, this strategy also has inherent limitations, such as difficulty in the detection of interactions with membrane proteins, large protein complexes, or protein-protein interactions that require in planta posttranslational modification (Brückner et al., 2009). These limitations are particularly relevant to G protein signaling, which classically couples to plasma membrane-localized receptors (G protein receptors [GPCRs]). Plant genomes encode only one sequence and structural homolog, GCR1, to mammalian GPCRs (Taddese et al., 2014), which are seven-transmembrane domain proteins (Pandey and Assmann, 2004; Fredriksson and Schiöth, 2005). In recent years, receptor-like kinases (RLKs) have been implicated as coupling with G protein signaling by genetic analysis, and a handful of reports have found physical interactions between specific RLKs and Gα (Bommert et al., 2013; Aranda-Sicilia et al., 2015; Liang et al., 2016) or Gβ (Ishida et al., 2014; Liang et al., 2016; Yu et al., 2016) in targeted immunoprecipitation (IP) or bimolecular fluorescence complementation (BiFC) assays.

In this study, we isolated in planta AGB1-associated proteins by coimmunoprecipitation (co-IP) and identified them by mass spectrometry. We found two RLKs present in multiple AGB1 immunoprecipitates: FERONIA (FER) and MDIS1-INTERACTING RECEPTOR LIKE KINASE2 (MIK2). FER is one of 17 members of the *Catharanthus roseus* RLK1-like subfamily of RLKs in Arabidopsis (Lindner et al., 2012). The Rapid Alkalinization Factor (RALF) family of ~35 peptides are ligands for the FER receptor, which have conserved roles in alkalinization of the apoplast and inhibition of cell expansion (Haruta et al., 2014; Murphy and De Smet, 2014; Stegmann et al., 2017). RALF1 is the best-studied member of the RALF family, and exogenous treatment with RALF1 has been shown to stimulate changes to the phosphorylation status of FER and other proteins (Haruta et al., 2014). We confirmed physical interaction between AGB1 and FER by BiFC. We then identified a new role of RALF1 in stomatal movement regulation.

We further demonstrated that AGB1, AGGs, and XLGs, rather than the canonical Gα, GPA1, participate in RALF1 control of stomatal movement.

RESULTS

Identification of AGB1-Associated Proteins by Co-IP and Mass Spectrometry

To date, Y2/3H screening has been the primary method used to identify AGB1 interactors (Mudgil et al., 2009; Kobayashi et al., 2012; Tsugama et al., 2012, 2013; Kansup et al., 2013, 2014; Xu et al., 2015). In order to identify AGB1-associated proteins in planta, we performed co-IP from transgenic Arabidopsis expressing 35S-driven FLAG-tagged AGB1 in the *agb1-2* background or from wild-type plants as a negative control. Previous studies showed that 35S::AGB1-GFP is localized mainly at the plasma membrane and in the nucleus (Anderson and Botella, 2007) and that AGB1 forms heterotrimers with Gαs and Gγs at the cell periphery in *Nicotiana benthamiana* in BiFC assays (Gookin and Assmann, 2014; Chakravorty et al., 2015). Consistent with the previous findings, we also found by immunoblot that AGB1 is enriched in the plasma membrane fraction (Supplemental Fig. S1). In order to reduce contamination from nonspecific binding of abundant proteins, a plasma membrane-enriched protein fraction was adopted for co-IP. The mild detergent *n*-dodecyl β-D-maltoside (DDM; 1%) was applied to solubilize membrane proteins and also to minimize the dissociation of protein complexes. Tandem mass spectrometry (MS/MS) was used to identify AGB1-associated proteins in the immunoprecipitates.

The following criteria were used for the designation of candidate positive interactors: (1) proteins not present in any of the negative control samples (wild-type Arabidopsis); (2) proteins with an unused score generated from ProteinPilot software of 1.3 or above (greater than 95% confidence interval for protein identification); (3) proteins localized to the plasma membrane, cytosol, and/or nucleus based on TAIR Gene Ontology component annotation; and (4) proteins not classified as commonly identified contaminants, which include heat shock proteins, ribosomal proteins, and translation and elongation factors (Trinkle-Mulcahy et al., 2008). Based on the above criteria, a total of 103 candidate AGB1-associated proteins were identified (Supplemental Tables S1–S4). Although the experiment was initially targeted to identify AGB1-associated proteins induced by salt stress (see "Materials and Methods"), we found that most of the associated proteins were present in both control and salt-treated samples and that there were no quantitative differences in the number of the 95% confident peptides between nonsalt and salt-treated samples (Supplemental Table S1). Therefore, we pooled the interactor candidates from different conditions and replicates and then further focused on the 32 proteins present at least twice with high confidence among different samples (Table I).

The most confidently identified proteins (with high unused scores) and proteins with the highest frequency of occurrence across different replicates were G protein subunits. All of the Gγ subunits (AGG1, AGG2, and AGG3) were identified. The canonical Gα subunit GPA1 and the extra-large Gα subunits XLG2 and XLG3 also were identified (Table I). These results lend credence to the protocol used, since all of the G-protein subunits are confirmed by other assays to interact with AGB1 (Gookin and Assmann, 2014; Chakravorty et al., 2015). In addition to the G protein subunits, we also identified RLKs, Ca^{2+}- or calmodulin-binding proteins, 14-3-3-like proteins, transporters, and other signaling proteins that may be involved in G protein signaling (Table I).

FER Interacts with Gβγ in BiFC Assays

Two RLKs, FER (AT3G51550) and MIK2 (AT4G08850), were identified at least twice in our co-IP assays (Table I). Interestingly, much like G proteins, FER has been shown to play roles in multiple processes, including ABA regulation of stomatal apertures (Wang et al., 2001; Fan et al., 2008; Yu et al., 2012; Chen et al., 2016). Therefore, we decided to further study the relationship between FER and G protein signaling.

An identified protein from a co-IP indicates that the two proteins exist together in a complex but does not evaluate direct interaction (Xing et al., 2016). To test whether FER interacts directly with G protein subunits, BiFC assays were performed in *N. benthamiana* utilizing our improved pDOE BiFC system with multiple cloning cassettes and reduced nonspecific signals (Gookin and Assmann, 2014). Full-length FER was initially inserted into MCS1 of BiFC vectors to generate FER-NVenus210 parent vectors as negative controls. However, transient expression of the parent vectors in *N. benthamiana* leaves resulted in cell death and autofluorescence, possibly due to the defense response elicited by FER (Keinath et al., 2010; Stegmann et al., 2017). Therefore, the C terminus (amino acids 469–895) of *FER* (*FERCT*), which retains autophosphorylation activity, and a kinase-inactive version of *FER* (*FERK565R*), in which Lys at position 565 is substituted for Arg (Escobar-Restrepo et al., 2007), were used for BiFC assays. We found that expressing the *FERCT* parent vector at a low infiltration OD_{600} (0.008) reduced cell damage and that expressing *FERK565R* completely suppressed cell damage. To determine which G protein subunits FER interacts directly with, we tested FERK565R and FERCT against all Gβγ combinations and all four Gα subunits (GPA1, XLG1, XLG2, and XLG3). G protein β and γ subunits operate as a noncovalent dimer, and previously, we found that coexpression of AGGs with AGB1 facilitates the interaction between GPA1 and AGB1 (Gookin and Assmann, 2014). Accordingly, untagged *AGG1*, *AGG2*, *AGG3*, or *AGG1/AGG2* were coinfiltrated with the *FERCT/FERK565R-NVenus210::CVenus-AGB1* vector in BiFC

assays. The Golgi-localized mTurquoise marker (blue punctate structures) indicates successful transformation (Fig. 1; Supplemental Fig. S3; Gookin and Assmann, 2014). No clear signal was observed in the negative control (Fig. 1, A and F) or in the absence of AGGs (Fig. 1, B and G). In contrast, there was clear mVenus signal (yellow) at the cell periphery in samples expressing either FERK565R or FERCT with AGB1 in the presence of any of the AGGs (Fig. 1, C–E and H–J), indicating interaction. The quantification of BiFC signal is shown in Supplemental Figure S2. Neither FERK565R nor FERCT interacted with GPA1, XLG1, XLG2, or XLG3 (Supplemental Fig. S3).

A Ligand of FER, RALF1, Regulates Stomatal Movement, Which Requires AGB1 and AGGs

RALF1 is a polypeptide ligand of FER that increases external pH and inhibits growth (Pearce et al., 2001; Haruta et al., 2014; Murphy and De Smet, 2014). RALF1 directly binds FER and promotes the phosphorylation of FER and other proteins (Haruta et al., 2014). *RALF1* is highly expressed in roots (Haruta et al., 2014). Our RT-PCR analysis as well as published microarray data show that RALF1 also is expressed in guard cells (Supplemental Fig. S4; Pandey et al., 2010). Both FER and G proteins are involved in the modulation of the guard cell ABA response (Wang et al., 2001; Fan et al., 2008; Yu et al., 2012; Chen et al., 2016); however, a function of RALF1 in stomatal regulation had never been investigated. Therefore, we first explored the effects of RALF1 on stomatal movement by applying 10 μM active RALF1. As negative controls, we included treatments with buffer only or an inactive RALF1 analog, RALF1Δ (a deletion of amino acids 2–8), that does not activate the FER receptor (Haruta et al., 2014). As shown in Figure 2, RALF1 inhibits stomatal opening and promotes stomatal closure, whereas RALF1Δ did not show any effect, similar to the buffer-only control. We subsequently found that 1 μM RALF1, which is the RALF1 concentration most often used in physiological assays (Haruta et al., 2008, 2014; Li et al., 2015; Stegmann et al., 2017), is sufficient to regulate stomatal apertures in Col (Fig. 3, A and B). The RALF1 effect was completely lost in the *fer-2* and *fer-4* mutants, confirming that the RALF1 ligand affects stomatal apertures through the FER receptor (Fig. 3; Supplemental Fig. S5).

As AGB1 and FER exist in a complex and interact directly in our BiFC assays (Table I; Fig. 1), we next investigated whether AGB1 mediates the RALF1 effect on stomatal movement. *agb1-2* exhibits insensitivity to 1 μM RALF1 (Fig. 3, A and B). We also tested *agb1-2* as well as another independent *agb1* mutant, *agb1-9*, at a 10-fold higher concentration of RALF1 (10 μM) and again observed insensitivity, or occasional hyposensitivity, in stomatal opening and closure assays (Figs. 3, C and D, and 4). These results suggest that AGB1 is necessary to transduce the RALF1 signal. *agb1-2 fer-2* double mutants were insensitive to RALF1, as

Table I. *AGB1-associated proteins present in multiple AGB1 co-IP and mass spectrometry assays*

AGB1 co-IP was performed using full rosettes of *agb1-2 35S::FLAG-AGB1* transgenic plants. Multiple replicates were pooled together for the analyses of candidate proteins. Listed proteins meet all the criteria defined in the text.

Gene Locus	Protein Name	Occurrence/Total No. of Experiments	Implications in G Protein Signaling
Heteromeric G proteins			
AT3G63420	Guanine nucleotide-binding protein subunit $\gamma 1$	9/9	G protein subunit
AT3G22942	Guanine nucleotide-binding protein subunit $\gamma 2$	9/9	G protein subunit
AT5G20635	Guanine nucleotide-binding protein subunit $\gamma 3$	7/9	G protein subunit
AT2G26300	Guanine nucleotide-binding protein α-1 subunit	8/9	G protein subunit
AT1G31930	Extra-large GTP-binding protein3	5/9	G protein subunit
AT4G34390	Extra-large GTP-binding protein2	3/9	G protein subunit
Receptor-like kinases			
AT4G08850	MDIS1-INTERACTING RECEPTOR-LIKE KINASE2, MIK2	4/9	RLKs interact with G protein subunits (Bommert et al., 2013; Ishida et al., 2014; Liang et al., 2016; Yu et al., 2016)
AT3G51550	Receptor-like protein kinase FERONIA	2/9	RLKs interact with G protein subunits (Bommert et al., 2013; Ishida et al., 2014; Liang et al., 2016; Yu et al., 2016)
Ca^{2+} or calmodulin binding			
AT2G41110	Calmodulin2	2/9	
AT2G38750	Annexin D4	2/9	ANNEXIN1 (AT1G35720) interacts with AGB1 and RGS1 (Klopffleisch et al., 2011)
AT1G74690	IQ-domain 31 protein	2/9	IQD6 (AT2G26180) interacts with AGB1 (Jones et al., 2014)
14-3-3-like proteins			
AT1G35160	14-3-3-like protein GF14 phi	3/9	14-3-3-like protein GF14 PHI (AT1G35160) interacts with RGS1 (Jaiswal et al., 2016)
AT4G09000	14-3-3-like protein GF14 chi	2/9	14-3-3-like protein GF14 PHI (AT1G35160) interacts with RGS1 (Jaiswal et al., 2016)
Transporters and channels			
AT1G70940	Auxin efflux carrier component3	2/9	Auxin signaling (Ullah et al., 2003)
AT4G35100	Plasma membrane intrinsic protein3	2/9	PIP2;1 (AT3G53420) interacts with RGS1 (Jaiswal et al., 2016)
Unfolded protein binding			
AT5G20890	TCP-1/cpn60 chaperonin family protein	3/9	
AT3G03960	TCP-1/cpn60 chaperonin family protein	2/9	
AT3G18190	TCP-1/cpn60 chaperonin family protein	2/9	
AT3G11830	TCP-1/cpn60 chaperonin family protein	2/9	
AT3G20050	T-complex protein1 subunit α	2/9	
Metabolic enzymes			
AT3G07020	Sterol 3β-glucosyltransferase	4/9	
AT2G30860	GST PHI9	2/9	
AT2G29560	Putative phospho*enol*pyruvate enolase	2/9	
ATP binding			
AT3G50950	Protein HOPZ-ACTIVATED RESISTANCE1	2/9	
AT3G28520	AAA-type ATPase family protein	2/9	
Tetratricopeptide family proteins			
AT2G32450	Tetratricopeptide repeat-containing protein	2/9	

Table I. (*Continued from previous page.*)

Gene Locus	Protein Name	Occurrence/Total No. of Experiments	Implications in G Protein Signaling
AT4G28080	Tetratricopeptide repeat domain protein	2/9	
Phosphatidylinositol phosphorylation			
AT1G49340	Phosphatidylinositol 4-kinase α	2/9	
mRNA processing			
AT5G52040	Arg/Ser-rich-splicing factor RSP41	2/9	
Actin related			
AT1G30825	Actin-related protein C2A	2/9	
Defense response related			
AT5G06320	NDR1/HIN1-like protein3	4/9	Defense response (Trusov et al., 2006)
Endoplasmic reticulum related			
AT3G10260	Reticulon-like protein B8	3/9	

expected for a RALF1 receptor mutant (Fig. 3). Since Gβ responses are mediated by G$\beta\gamma$ dimers (Thung et al., 2012), we also tested *agg1 agg2 agg3* triple mutants for RALF1 stomatal responses. Similar to *agb1*, *agg* triple mutants were insensitive to RALF1 in both stomatal opening and closure assays (Fig. 4).

Extra-Large G Proteins Participate in RALF1 Regulation of Stomatal Movement

Recent studies suggest that GPA1 and the non-canonical Gα subunits XLGs partition or compete in different physiological responses in G protein signaling (Chakravorty et al., 2015; Urano et al., 2016a). We next investigated whether GPA1 or XLGs were required for RALF1 regulation of guard cell signaling. Interestingly, *gpa1* mutants retained sensitivity to RALF1 in both inhibition of stomatal opening and promotion of stomatal closure. In contrast, the *xlg* triple mutants showed insensitivity to RALF1 in both stomatal opening and stomatal closure (Fig. 4). *gpa1 xlg1 xlg2 xlg3* quadruple mutants showed similar phenotypes to the *agb1* and *xlg* triple mutants (Fig. 4), further supporting the absence of a major role for GPA1 in RALF1 stomatal responses.

RALF1 Inhibition of Stomatal Opening Requires OST1

FER interacts directly with ABA signaling components, including the A-group protein phosphatases type 2C (PP2Cs), ABA INSENSITIVE1 (ABI1), ABI2, HYPERSENSITIVE TO ABA1 (HAB1), and HAB2 (Chen et al., 2016). PP2Cs are inhibited by ABA-bound PYR/RCAR receptors, and active PP2Cs inhibit the downstream SNF-RELATED PROTEIN KINASE2s (SnRK2s), including SnRK2.6/OPEN STOMATA1 (OST1; Hubbard et al., 2010). To investigate whether these ABA signaling components downstream of FER also play roles in the transduction of the RALF1 signal in guard cells, *ost1* mutants were assayed in stomatal movement response. *ost1-1* and *ost1-2* were hyposensitive to the RALF1 inhibition of stomatal opening (Fig. 5A) but showed a wild-type response to RALF1 promotion of stomatal

closure (Fig. 5B), suggesting that the RALF1 effect on stomatal opening and closure is mediated by different components and that OST1 is only involved in the stomatal opening response.

To assess whether G proteins play roles in FER-PP2C-OST1 signaling, we assayed potential protein-protein interactions between AGB1 and ABA signaling proteins using BiFC assays. The Golgi-localized mTurquoise marker (blue punctate structures) was well expressed, indicating efficient transformation (Fig. 6). No mVenus signal was observed in the control (Fig. 6A) or in BiFC vectors of AGB1 tagged with the N terminus of mVenus and tested against OST1 or ABI1 tagged with the C terminus of mVenus in either the absence of AGGs (Fig. 6, B and E) or the presence of AGG3 (Fig. 6, C and F). Conversely, we observed positive mVenus signal in BiFC in the presence of additional AGG1/AGG2 (Fig. 6, D and G), indicating that AGB1 interaction with OST1 and ABI1 requires the presence of AGG1 and/or AGG2, as would be expected given that Gβ and Gγ subunits are known to function as nondissociable dimers. We also observed weak mVenus signal in BiFC between AGB1 and ABI2 in the presence of AGG1/2 (Supplemental Fig. S6C), with higher intensity than the signal in AGB1 and ABI2 samples with no AGGs present (Supplemental Fig. S6A), indicating plausible interaction between AGB1 and ABI2 in the presence of AGG1/2. No BiFC signal was observed between AGB1 and ABI2 in the presence of AGG3 (Supplemental Fig. S6B).

Together, these results suggest that FER, G protein subunits (XLGs, AGB1, and AGGs), and well-known ABA signaling components (OST1, ABI1, and possibly ABI2) constitute a guard cell signaling cascade that is activated by RALF1.

DISCUSSION

Co-IP Provides New Insights on the G Protein Interactome

The G protein interactome mainly has been investigated using Y2/3H methods, including library screening (Lapik and Kaufman, 2003; Huang et al., 2006; Mudgil et al., 2009; Klopffleisch et al., 2011). Only
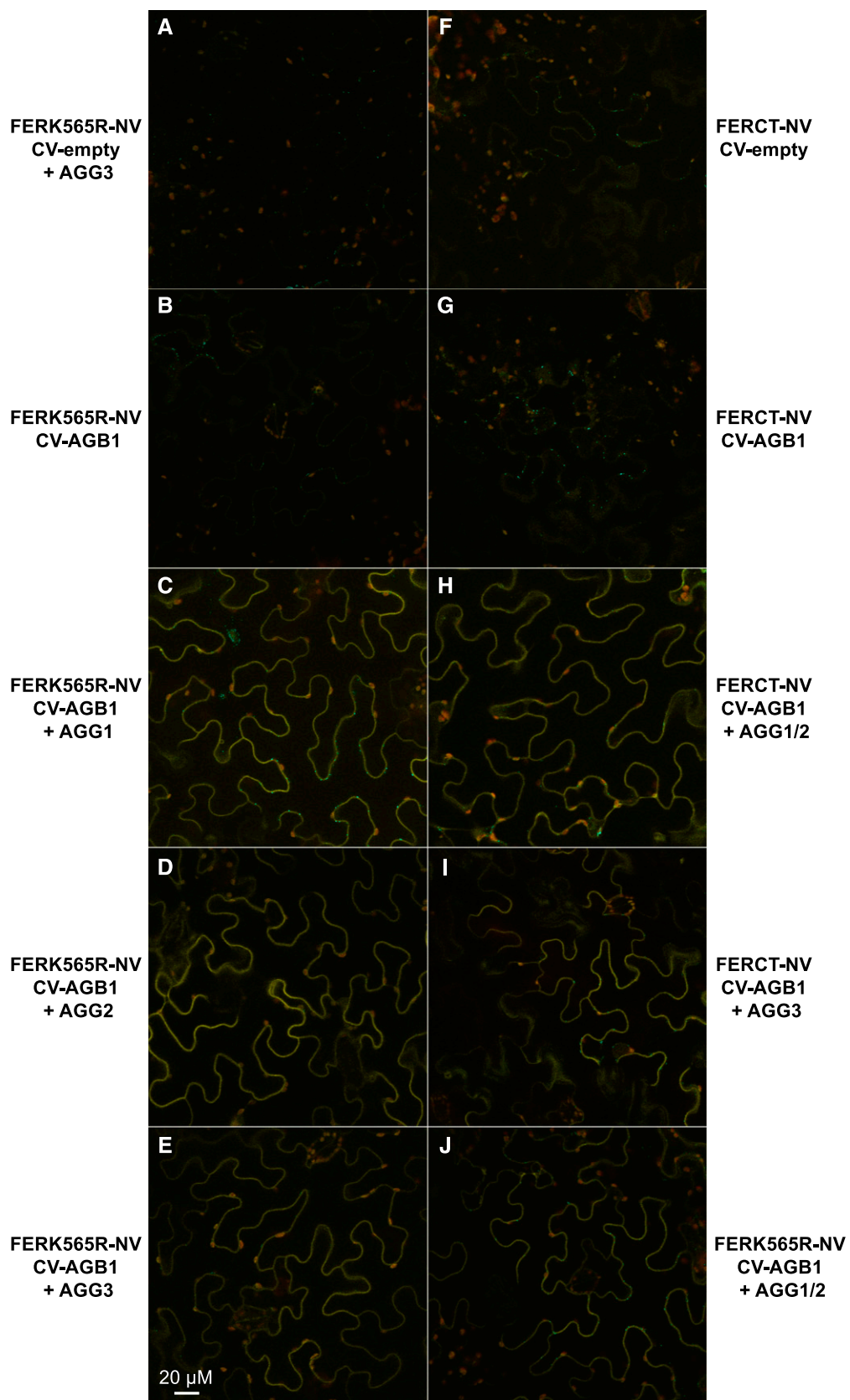
Figure 1. FER interacts with AGB1 in the presence of AGGs. BiFC assays were performed using the pDOE vector system with Golgi-localized mTurquoise2 as an indicator of positive transformation. *Agrobacterium tumefaciens* was infiltrated at an OD_{600} of 0.008 for each construct, and images were taken ~60 h after infiltration. Yellow = mVenus BiFC, blue = mTurquoise2 Golgi marker indicator, and red = chloroplast autofluorescence. A and F, Signals of the parent vectors of FERK565R (A) or FERCT (F) tagged with the N terminus of mVenus in the presence or absence of additional AGG3. B
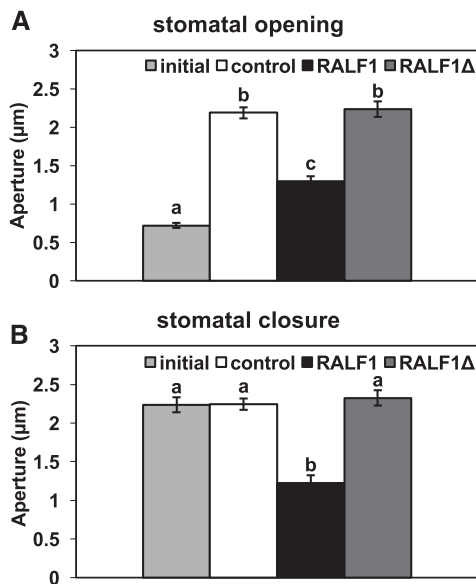
A
stomatal opening

B
stomatal closure

Figure 2. RALF1 inhibits stomatal opening and promotes stomatal closure. A, RALF1 inhibition of stomatal opening in Col. Leaf pieces were incubated in the dark to close the stomata for 2 h and then treated with or without 10 μM RALF1 or RALF1Δ in the light for another 3 h. B, RALF1 promotion of stomatal closure in Col. Leaf pieces were incubated in the light for 3 h to open the stomata and then treated with or without 10 μM RALF1 or RALF1Δ in the light for another 2 h. The results are means $\pm$ SE for three independent experiments with over 80 apertures measured per genotype per treatment. Significant differences between conditions (Student's t test, $P < 0.05$) are indicated with different letters.

recently, an interactome of Regulator of G-protein Signaling1 (RGS1) upon time-dependent Glc treatment was profiled using co-IP followed by mass spectrometry (Jaiswal et al., 2016). In our study, we aimed to identify the associated proteins of AGB1 in planta. Both our results (Supplemental Fig. S1) and previous studies (Obrdlik et al., 2000; Anderson and Botella, 2007) showed that AGB1 is enriched in the plasma membrane fraction. Therefore, we chose to isolate the plasma membrane fraction for our IP, which also minimized contaminants from other cell compartments.

The most abundant interactors identified are G protein subunits (Table I; Supplemental Tables S1–S3), which is consistent with the formation of G$\beta\gamma$ dimers or G$\alpha\beta\gamma$ heterotrimers in G protein signaling. Among the other interacting candidates (Table I), some of the novel interactors have been implicated in G protein pathways. For example, ANNEXIN1, which is a homolog of ANNEXIN D4 (AT2G38750) found in this study,

interacts physically with AGB1 and RGS1 in Y2H and BiFC assays (Klopffleisch et al., 2011). IQD6, which is a homolog of IQD31 (AT1G74690) found in this study, interacts with AGB1 in Y2H assay (Jones et al., 2014). The 14-3-3-like protein GF14 PHI (AT1G35160) was found both in our experiments and as an RGS1-associated protein (Jaiswal et al., 2016). We also identified aquaporin PIP3 (AT4G35100), which is a homolog of the RGS1-associated protein PIP2;1 (Jaiswal et al., 2016). Interestingly, aquaporins also are associated with FER, which regulates the permeability of water channels through modulating the phosphorylation status of aquaporins (Bellati et al., 2016). Moreover, the auxin transporter PIN3 (AT1G70940) and a defense-related protein NDR/HIN1-LIKE3 (AT5G06320) found in this study (Table I) may be related to G protein-mediated auxin (Ullah et al., 2003; Mudgil et al., 2009) and defense responses (Llorente et al., 2005; Zhu et al., 2009; Liang et al., 2016).

Another group of AGB1 interactors that we found are RLKs, which recently were newly proposed as potential plant GPCRs (Trusov and Botella, 2016). Some RLKs have been shown to interact physically or genetically with either Gα or Gβ subunits. For example, the maize (*Zea mays*) Gα COMPACT PLANTS2 and CLAVATA RLK FASCIATED EAR2 appeared in the same protein co-IP complexes, and both control shoot apical meristem (SAM) development (Bommert et al., 2013). In Arabidopsis, null mutation of *AGB1* enhanced the enlarged SAM phenotype of the CLAVATA RLK mutants *clv1*, *clv2*, and *rpk2* (*receptor-like protein kinase2*). AGB1 has been shown by BiFC and co-IP to interact directly with RPK2 (Ishida et al., 2014). AGB1 also interacts physically with an RLK, ZAR1, which regulates zygote development (Yu et al., 2016). AGB1 and XLG2 are associated with RLKs in immunity responses. The null mutation of *AGB1* or *XLG2* partially rescues the seedling-lethal phenotypes of the defense RLK *bir1* (*brassinosteroid insensitive-associated receptor kinase1-interacting receptor-like kinase1*; Liu et al., 2013; Maruta et al., 2015). GPA1, AGG1, and AGG2, but not AGB1, interact physically with BIR1, BRI1-ASSOCIATED RECEPTOR KINASE, and CHITIN ELICITOR RECEPTOR KINASE1 in split ubiquitin and BiFC assays (Aranda-Sicilia et al., 2015). In addition, both AGB1 and XLG2 bind and stabilize BOTRYTIS-INDUCED KINASE1 for immune response activation (Liang et al., 2016).

In our study, we identified two RLKs in more than one independent AGB1 co-IPs, FER and MIK2 (Table I), which had not been implicated previously as coupling with heterotrimeric G proteins. We confirmed that FER

Figure 1. (*Continued.*)
and G, BiFC signals of FERK565R (B) or FERCT (G) tagged with the N terminus of mVenus and AGB1 tagged with the C terminus of mVenus in the absence of additional untagged AGGs. C to E and J, BiFC signals of FERK565R tagged with the N terminus of mVenus and AGB1 tagged with the C terminus of mVenus in the presence of additional untagged AGG1 (C), AGG2 (D), AGG3 (E), or AGG1/AGG2 (J). H and I, BiFC signals of FERCT tagged with the N terminus of mVenus and AGB1 tagged with the C terminus of mVenus in the presence of additional untagged AGG1/AGG2 (H) or AGG3 (I).
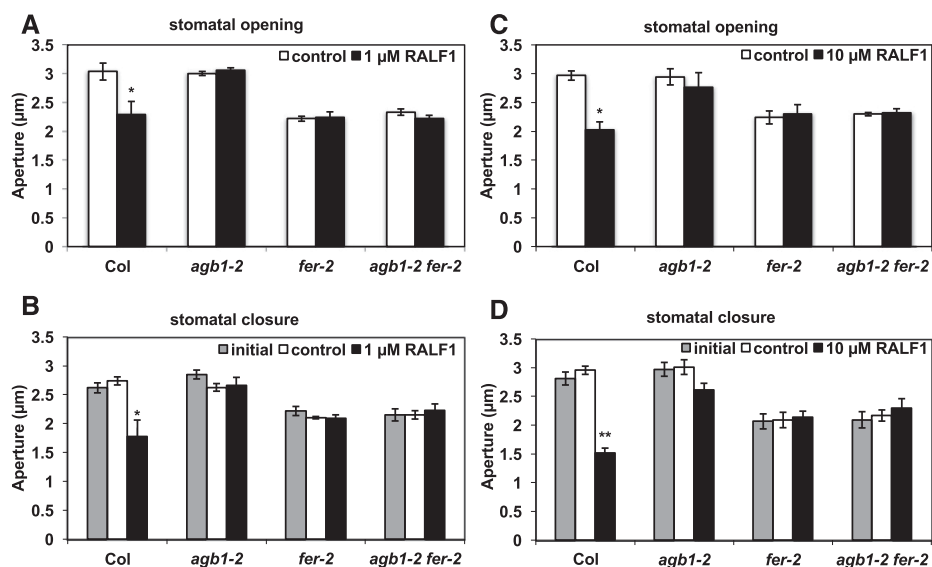
Figure 3. RALF1 affects stomatal movement in an AGB1- and FER-dependent manner. A and C, RALF1 inhibition of stomatal opening in Col, *agb1-2*, *fer-2*, and *agb1-2 fer-2*. Leaf pieces were incubated in the dark to close the stomata for 2 h and then treated with or without 1 μM (A) or 10 μM (C) RALF1 in the light for another 3 h. B and D, RALF1 promotion of stomatal closure in Col, *agb1-2*, *fer-2*, and *agb1-2 fer-2*. Leaf pieces were incubated in the light for 3 h to open the stomata and then treated with or without 1 μM (B) or 10 μM (D) RALF1 in the light for another 2 h. The results are means ± SE for three or four independent experiments with over 80 apertures measured per genotype per treatment. Significant differences between control and treatment (Student's *t* test) are indicated with asterisks (*, $P < 0.05$ and **, $P < 0.01$).

interacts directly with AGB1 rather than the Gαs (GPA1, XLG1, XLG2, or XLG3; Fig. 2; Supplemental Figs. S2 and S3). In addition to FER and MIK2, we also identified three other RLKs (AT5G39000, AT1G48480, and AT5G3410) in single co-IP experiments (Supplemental Tables S1–S3).

RALF1 May Regulate Stomatal Opening and Closure through Distinct Pathways

Consideration of the cellular mechanisms underlying stomatal movement regulation may provide some clues regarding the guard cell pathways activated by RALF1. Stomatal movement is mediated through changing osmotic pressure of paired guard cells by osmotica such as K$^+$ and anions (Fan et al., 2004). Light-induced stomatal opening is driven mainly by activation of the plasma membrane H$^+$-ATPase, which hyperpolarizes the plasma membrane and provides a driving force for K$^+$ uptake via inwardly rectifying K$^+$ channels (Fan et al., 2004), while stomatal closure involves Ca^{2+} and reactive oxygen species elevation and the activation of outwardly rectifying K$^+$ channels and anion channels (Pei et al., 2000; Kwak et al., 2003). During guard cell ABA responses, the OST1 kinase is activated by autophosphorylation as a result of relief from inhibition by PP2C phosphatases. The OST1 kinase targets multiple downstream effectors, including the inwardly rectifying K$^+$ channel, KAT1 (Sato et al., 2009; Acharya et al., 2013), which mediates K$^+$ uptake during stomatal

opening. *ost1* mutants are impaired in both ABA inhibition of stomatal opening and ABA promotion of stomatal closure (Mustilli et al., 2002). By contrast, we found that RALF1 inhibits stomatal opening in an OST1-dependent manner (Fig. 5A) but promotes stomatal closure in an OST1-independent manner (Fig. 5B), suggesting that RALF1 regulates stomatal opening and closure through signaling pathways that include distinct components.

RALF1 inhibits stomatal opening and promotes stomatal closure (Fig. 2). RALF1 activates FER and further modulates the phosphorylation status of FER and downstream signaling components, including AHA2 and CPK9 (Haruta et al., 2014). AHA2 may be involved in the RALF1 regulation of stomatal movement through regulating the hyperpolarization of the plasma membrane, which provides a driving force for cation uptake. Interestingly, AHA phosphorylation induced by blue light is normal in *abi1-1*, *abi2-1*, and *ost1-2* mutants, suggesting that the blue light-induced AHA phosphorylation is independent of the core ABA signaling components (Hayashi et al., 2011). Additionally, RALF1 promotes transient cytosolic Ca^{2+} elevation in seedlings (Haruta et al., 2008), and elevated cytosolic Ca^{2+} is sufficient to promote stomatal closure (Allen et al., 2001). Integrating our current data with these observations, we hypothesize that RALF1 stimulates stomatal closure through cytosolic Ca^{2+} signaling, while RALF1 inhibits stomatal opening by an OST1-dependent mechanism. In addition, AHA2 may participate in RALF1 signaling by the regulation of plasma
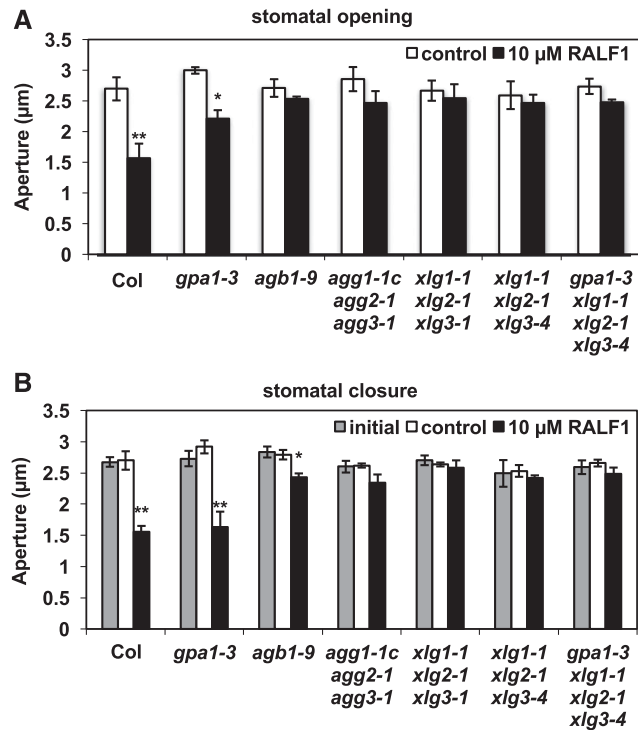
Figure 4. AGGs and XLGs are involved in RALF1 inhibition of stomatal opening and RALF1 promotion of stomatal closure. A, RALF1 inhibition of stomatal opening in G protein mutants. Leaf pieces were incubated in the dark to close the stomata for 2 h and then treated with or without 10 μM RALF1 in the light for another 3 h. B, RALF1 promotion of stomatal closure in G protein mutants. Leaf pieces were incubated in the light for 3 h to open the stomata and then treated with or without 10 μM RALF1 in the light for another 2 h. The results are means ± SE for three independent experiments with over 80 apertures measured per genotype per treatment. Significant differences between control and treatment (Student's *t* test) are indicated with asterisks (*, $P < 0.05$ and **, $P < 0.01$).

membrane hyperpolarization (Fig. 7). While RALF1 has received the most attention in the literature (Haruta et al., 2014; Li et al., 2015; Chen et al., 2016) and so was the focus of our assays, we do not exclude the possibility that other RALF-like peptides also modulate stomatal apertures in a FER-dependent manner.

While it is customary to think of a ligand as activating a receptor, an alternative hypothesis consistent with our data is that FER promotes stomatal apertures in the absence of RALF1 application and that RALF1 negatively regulates FER in an AGB1-dependent manner. Thus, basal stomatal apertures are smaller in the *fer* mutant and also are smaller in RALF1-treated Col but not in RALF1-treated *agb1* (Figs. 2 and 3; Supplemental Fig. S5). A caveat concerning this alternative hypothesis is that the smaller basal apertures in *fer* arise from a developmental effect rather than a physiological response; however, we see a FER-dependent response to RALF1 application within a few hours, clearly indicating that FER and RALF1 play signaling, and not solely developmental, roles in guard cell physiology.

G Proteins Are Necessary for RALF1 Control of Stomatal Movement

Arabidopsis possesses one canonical Gα (GPA1; Ma et al., 1990) and three plant-specific extra-large Gα subunits (XLG1, XLG2, and XLG3; Lee and Assmann, 1999; Ding et al., 2008). We and others showed previously that GPA1 and the XLGs may compete or partition in different aspects of G protein signaling (Chakravorty et al., 2015; Urano et al., 2016a). In ABA regulation of stomatal movement, while both the *gpa1* and *agb1* mutants show wild-type responses to ABA promotion of stomatal closure, they are both hyposensitive to ABA inhibition of stomatal opening (Wang et al., 2001; Fan et al., 2008). However, AGB1 and the XLGs, but not GPA1, are required for RALF1 regulation of both stomatal opening and stomatal closure (Fig. 4), indicating the partitioning of roles between GPA1 and the XLGs in ABA versus RALF1 regulation of guard cell responses.
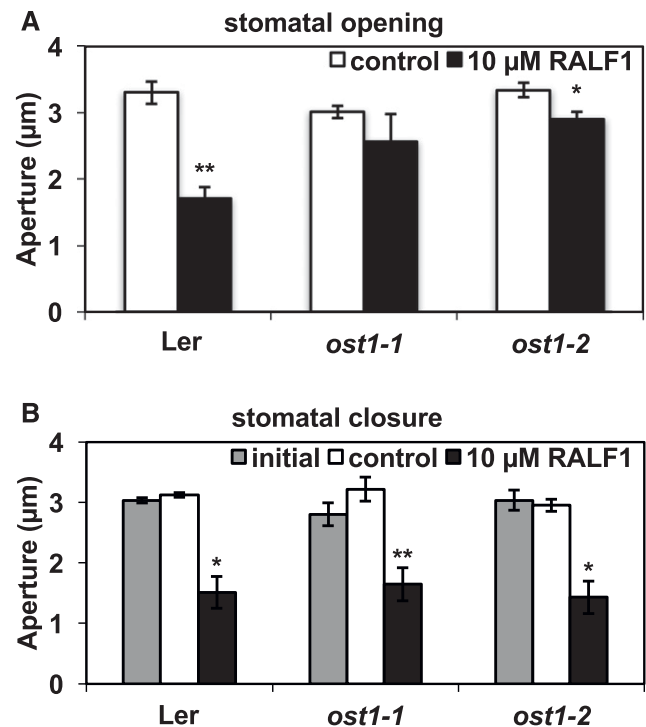

Figure 5. OST1 participates in RALF1 inhibition of stomatal opening but not RALF1 promotion of stomatal closure. A, RALF1 inhibition of stomatal opening in Landsberg *erecta* (L*er*) and *ost1* mutants. Leaf pieces were incubated in the dark to close the stomata for 2 h and then treated with or without 10 μM RALF1 in the light for another 3 h. B, RALF1 promotion of stomatal closure in L*er* and *ost1* mutants. Leaf pieces were incubated in the light for 3 h to open the stomata and then treated with or without 10 μM RALF1 in the light for another 2 h. The results are means ± SE for three independent experiments with over 80 apertures measured per genotype per treatment. Significant differences between control and treatment (Student's *t* test) are indicated with asterisks (*, $P < 0.05$ and **, $P < 0.01$).
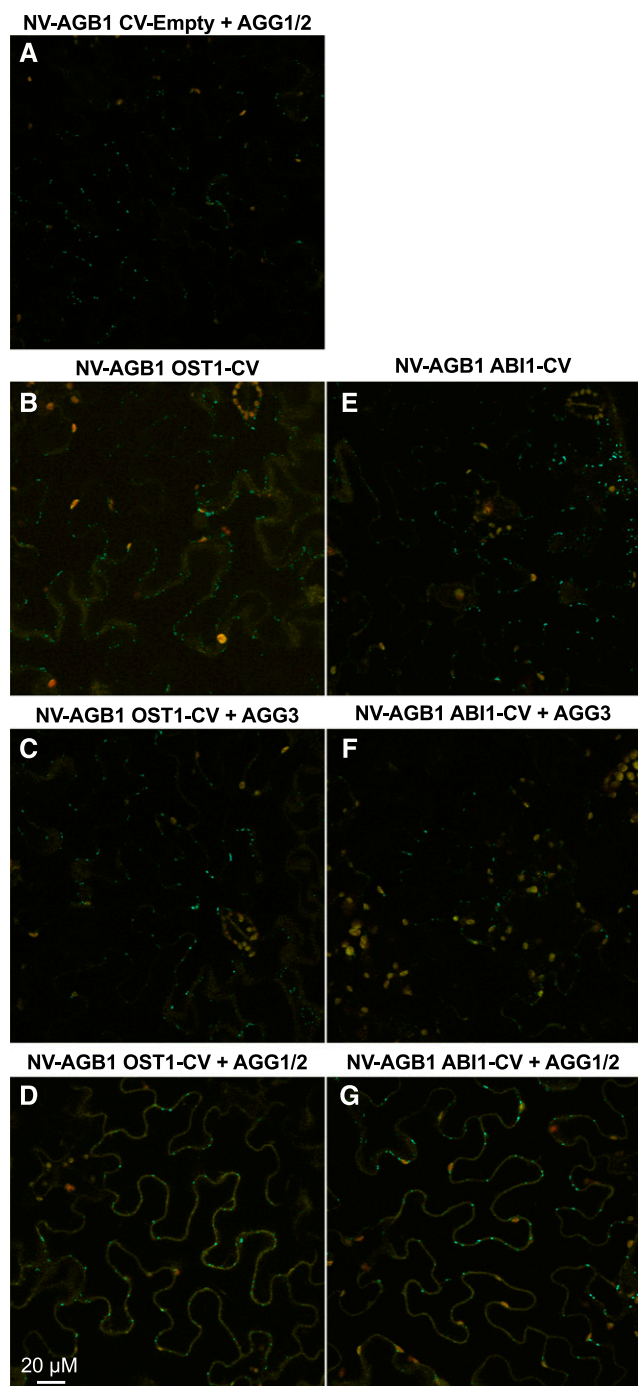
Figure 6. AGB1 interacts in BiFC with ABA signaling components in the presence of AGG1/AGG2. BiFC assays were performed using the pDOE vector system with Golgi-localized mTurquoise2 as an indicator of positive transformation. *A. tumefaciens* was infiltrated at an OD_{600} 0.02 for each construct, and images were taken ~60 h after infiltration. Yellow = mVenus BiFC, blue = mTurquoise2 Golgi marker, and red = chloroplast autofluorescence. A, Signals of the parent vectors of AGB1 tagged with the N terminus of mVenus in the presence of additional AGG1/AGG2. B and E, BiFC signals of AGB1 tagged with the N terminus of mVenus and OST1 (B) or ABI1 (E) tagged with the C terminus of mVenus in the absence of additional untagged AGGs. C and F, BiFC signals of AGB1 tagged with the N terminus of mVenus and OST1 (C) or

The cross talk between ABA and RALF1-FER signaling may be mediated in part by modulation of the phosphorylation status of FER by ABI2 (Chen et al., 2016). A previous study showed that AGB1 interacts with PP2C52 in the Y2H assay (Tsugama et al., 2012). We further showed that Gβγ interacts with ABI1 and OST1 in BiFC (Fig. 6), providing a possible mechanism by which Gβγ transduces the RALF1 signal to core guard cell signaling elements (Fig. 7). The phosphorylation status of OST1 is regulated by both autophosphorylation and the activity of PP2C phosphatases (Hubbard et al., 2010). It would be interesting to test whether, during the inhibition of stomatal opening, RALF1 promotes the phosphorylation of OST1 in a Gβγ-dependent manner.

According to our proposed model (Fig. 7), cytosolic Ca^{2+} signaling and the plasma membrane H^+-ATPase may be downstream mediators in RALF1 regulation of stomatal responses. Phosphorylation of the plasma membrane H^+-ATPase is stabilized by 14-3-3-like proteins (Olsson et al., 1998; Kinoshita and Shimazaki, 1999). Interestingly, Ca^{2+} signaling proteins are present in the set of AGB1-associated proteins (Table I), and the 14-3-3-like protein GF14 PHI is present in both AGB1 (Table I) and RGS1-associated protein complexes (Jaiswal et al., 2016). These observations provide potential candidates downstream of FER-RALF signaling mediated by G proteins. We occasionally saw a hyposensitivity of *agb1-9* in response to high concentrations of RALF1 (Fig. 4B). However, it should be noted that the *agb1-9* mutant contains an ethyl methanesulfonate-induced point mutation that introduces a premature stop codon late in the open reading frame (Galvez-Valdivieso et al., 2009), and some phenotypes of this line have been observed to be appreciably weaker than for the *agb1-2* T-DNA null mutant (Lorek et al., 2013). Alternatively, additional signaling components may substitute to partially retain RALF1 signaling in G protein mutant guard cells. The phenomenon that *rlk* mutants show more severe phenotypes than G protein mutants also was observed in SAM development (Bommert et al., 2013; Ishida et al., 2014) and defense signaling (Maruta et al., 2015).

CONCLUSION

This study identified novel candidate interactors of AGB1 using co-IP and mass spectrometry. One of the candidates, the RLK FER, was confirmed to interact directly with all three Gβγ dimers. Additionally, we demonstrated a new G protein-dependent function of RALF1 in the regulation of stomatal movement, with downstream components that are shared with the

ABI1 (F) tagged with the C terminus of mVenus in the presence of additional untagged AGG3. D and G, BiFC signals of AGB1 tagged with the N terminus of mVenus and OST1 (D) or ABI1 (G) tagged with the C terminus of mVenus in the presence of additional untagged AGG1/AGG2.

A RALF1 inhibition of stomatal opening
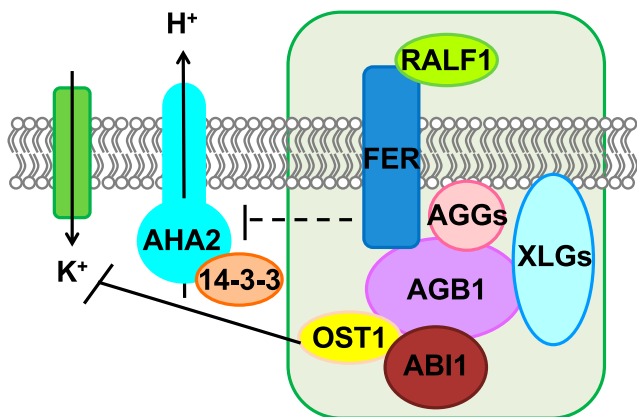
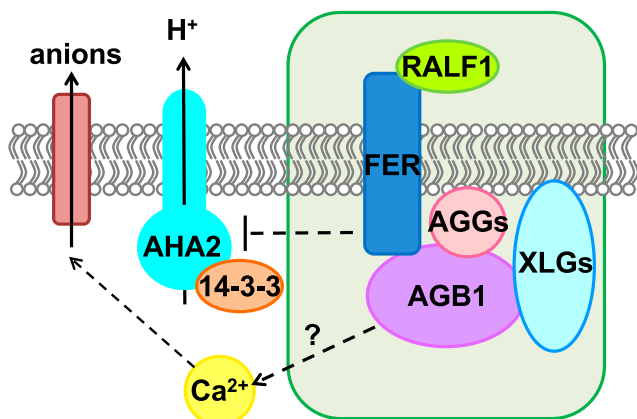## B RALF1 promotion of stomatal closure

Figure 7. Model of RALF1-FER regulation of stomatal movement via heterotrimeric G proteins and core ABA signaling components. The components in the green-shaded region are results from this work. A, RALF1 inhibits stomatal opening. AGB1/AGGs interact with FER; AGB1, AGGs, and XLGs play positive roles in RALF1 inhibition of stomatal opening. AGB1/AGGs also interact with the ABA signaling components, ABI1 and OST1. OST1 phosphorylates and inhibits the activity of the inwardly rectifying K^+ channel KAT1 (Sato et al., 2009; Acharya et al., 2013), resulting in the inhibition of stomatal opening. The RALF1 effect through FER also results in increased phosphorylation of the plasma membrane (PM) H^+-ATPase AHA2, which likely leads to the inhibition of AHA2 activity (Haruta et al., 2014). Active AHA hyperpolarizes the PM, which promotes K^+ influx via inwardly rectifying K^+ channels and, thus, stimulates stomatal opening (Fan et al., 2004). AHA proteins also are stabilized by binding with 14-3-3-like proteins (Olsson et al., 1998; Kinoshita and Shimazaki, 1999), which are present in AGB1-associated protein complexes. B, RALF1 promotion of stomatal closure requires AGB1/AGGs/XLGs but does not require OST1. RALF1 activation of FER may induce cytosolic Ca^{2+} elevation (Haruta et al., 2008), which promotes stomatal closure (Allen et al., 2001). Inhibition of PM H^+-ATPase activity depolarizes the PM and promotes anion channel activity, which leads to stomatal closure (Fan et al., 2004).

well-studied guard cell ABA signaling pathway. Our results support the hypothesis that RLKs act as GPCRs in plants.

MATERIALS AND METHODS

Plant Material and Growth

The following mutants or transgenic lines used in this study are in the Col background of Arabidopsis (*Arabidopsis thaliana*) and were described previously: *agb1-2* (Ullah et al., 2003), *agb1-9* (Galvez-Valdivieso et al., 2009), *fer-2* (Deslauriers and Larsen, 2010), *fer-4* (Duan et al., 2010), *gpa1-3* (Jones et al., 2003), *agg1-1c agg2-1 agg3-1* (Chakravorty et al., 2015), and *xlg1-1 xlg2-1 xlg3-1* (Ding et al., 2008). *xlg3-4* (SALK_107656c) has an insertion at 526 bp at the first exon of *XLG3*. RT-PCR for a 614-bp fragment of the first exon of *XLG3* was performed to confirm the absence of expression of *XLG3* in the *xlg3* mutants using primers that flank both the *xlg3-1* and *xlg3-4* insertion points (Supplemental Fig. S7). The Gα quadruple mutant was made using *gpa1-3* and *xlg1-1 xlg2-1 xlg3-4* triple mutants. Double mutants of *agb1-2 fer-2* were made using *agb1-2* as the female parent. The *ost1-1* and *ost1-2* mutants are in the Ler background (Acharya et al., 2013). Plants were grown in a growth chamber with an 8-h-light/16-h-dark regime with light intensity of 125 μmol m^{-2} s^{-1} and temperature of 21°C during the light period and 19°C during the dark period. Seeds were initially sterilized, spread on agar plates with one-half-strength Murashige and Skoog medium, 1% Suc, and 0.8% agar (Sigma), and kept at 4°C in the dark for 48 h. Seedlings were grown on agar plates for 10 to 12 d and transferred into hydroponics (Yu and Assmann, 2015) or soil (1:1 mix of Metro Mix 360:Sunshine Mix LC1; Sun Gro Horticulture) for different experiments.

Membrane Protein Extraction, IP, and Trypsin Digestion

35S::FLAG-AGB1 was introduced into the pEarleyGate202 vector (Earley et al., 2006), and the construct was transformed into the *agb1-2* background of Arabidopsis using the floral dip method (Clough and Bent, 1998). Col or the T2 generation of *35S::FLAG-AGB1 agb1-2* grown hydroponically for 4 weeks (Yu and Assmann, 2015) was treated with 100 mm NaCl in one-quarter-strength Hoagland solution for 0, 2, or 12 h. Plasma membrane proteins were extracted and enriched using the two-phase partitioning method (Qiu et al., 2002; Alexandersson et al., 2008) with some modifications. Specifically, rosette leaves (60–80 g fresh weight) from each treatment were homogenized in a cold room (4°C) in 200 mL of homogenization buffer containing 50 mm HEPES-KOH (pH 7.4), 330 mm Suc, 5 mm EDTA (pH 7.8), 10% glycerol, 5 mm DTT, 0.6% polyvinylpyrrolidone (molecular weight, 10,000), 1 μg mL^{-1} pepstatin A, 3 μg mL^{-1} leupeptin, 1 mm PMSF, and 5 mm ascorbic acid. The homogenates were filtered through a nylon filter and centrifuged at 10,000g for 10 min using a Beckman Coulter Avanti J-25 centrifuge. The supernatant was then spun down at 30,000g for 50 min using a Beckman Coulter ultracentrifuge. The supernatant was kept as the cytosolic fraction, and the microsomal pellet was resuspended using a 5-mL precooled Dounce homogenizer in 5 mL of 330 mm Suc, 5 mm K$_2$HPO$_4$/KH$_2$PO$_4$ (pH 7.8), 3 mm KCl, 1 μg mL^{-1} pepstatin A, 1 μg mL^{-1} leupeptin, 2 mm DTT, 1 mm PMSF and 0.1 mm EDTA (pH 7.8). Nine grams of this homogenate was then added to 27 g of a phase mixture in a 50-mL centrifuge tube to obtain a final concentration of 6.1% PEG3350, 6.1% Dextran 500, 330 mm Suc, 5 mm K$_2$HPO$_4$/KH$_2$PO$_4$ (pH 7.8), and 3 mm KCl. The tube was mixed thoroughly and carefully by slowly inverting the tubes 30 times, placed on ice for 5 min, and then centrifuged using a swinging-bucket clinical centrifuge at 750g for 5 min at 4°C. The upper phase containing the plasma membrane fraction and the lower phase containing the microsome fraction were diluted at least 3-fold with 20 mm HEPES-KOH (pH 7.4), 330 mm Suc, 10% glycerol, and 2 mm DTT and centrifuged at 100,000g at 4°C for 1 h. The pellets, containing either plasma membrane or microsomal vesicles, were resuspended using a paint brush, solubilized in IP buffer (20 mm HEPES-KOH, pH 7.4, 100 mm NaCl, 5 mm MgCl$_2$, 5% glycerol, 1× cOmplete Protease inhibitor [Roche], 1 mm 4-aminobenzamidine dihydrochloride, 5 mm 4-aminobenzoic acid, 1 μg mL^{-1} pepstatin A, and 5 mm NaF) with 1% DDM for 20 min on a rotator at 4°C, and centrifuged at 100,000g at 4°C for 1 h, and the supernatant was removed to new 1.5-mL tubes.

Co-IP and subsequent trypsin digestion were modified from a previous method (Bommert et al., 2013). The solubilized plasma membrane proteins were diluted with IP buffer to obtain a final concentration of 0.25% DDM. IP was

immediately performed by incubating ~150 μg (600 μL) of proteins with 20 μL of ANTI-FLAG M2 Affinity Gel (Sigma) on a rotator for 2 h at 4°C.

After washing twice with IP buffer plus 0.2% DDM followed by two washes with 50 mM NH$_4$HCO$_3$, agarose beads with retained proteins were resuspended with 100 μL of 50 mM NH$_4$HCO$_3$, 0.01% ProteaseMax (Promega), and 1 M urea. Trypsin digestion was then performed by adding 1 μg of Trypsin Lys-C (Promega) and incubating at 37°C for 1 h with mild shaking (80 rpm). Then, the partially digested proteins were released from beads by eluting twice with 50 μL of 5 mM DTT in 50 mM NH$_4$HCO$_3$, 0.01% ProteaseMax, and 1 M urea, followed by 30 min of DTT reduction at 37°C in the dark. The samples were then alkalinized by adding iodoacetamide to a final concentration of 10 mM and subjected to continued digestion by Trypsin Lys-C overnight (~13 h) at 37°C in the dark. Digestion was terminated by adding trifluoroacetic acid to a final concentration of 0.5%.

Mass Spectrometric Analysis and Database Search

Peptides were lyophilized using a CentriVap −84°C cold trap (Labconco), desalted using Pierce C18 Tips (ThermoFisher), and then analyzed with a Sciex 5600 TripleTOF mass spectrometer at the Proteomics and Mass Spectrometry Core at Pennsylvania State College of Medicine in Hershey. Specifically, peptide samples were injected using an Eksigent NanoLC-Ultra-2D Plus system (ABSciex/Eksigent) in a 60-min gradient. Trap and elute mode was used for separation using the microfluidics on an Eksigent cHiPLC Nanoflex system equipped with a trap column (200 μm × 0.5 mm Chrom XP C18-CL, 3 μm, 120 Å) and a Nano cHIPLC column (75 μm × 15 cm Chrom XP C18-CL, 3 μm, 120 Å). The elution gradient was run at a 300 nL min^{-1} flow rate from 95% A (0.1% formic acid dissolved in water)/5% B (0.1% formic acid dissolved in acetonitrile) to 65% A/35% B over 60 min, followed by 15% A/85% B from 61 to 70 min, and then 95% A/5% B from 71 to 80 min.

The eluate was delivered into the mass spectrometer with a NanoSpray III source using a 10-μm i.d. nanospray tip (New Objective). Typical gas and other mass spectrometer settings were curtain gas 1 (nitrogen) = 10 and gas 3 (nitrogen) = 25. Each cycle consisted of a TOF-MS/MS spectra acquisition for 250 ms followed by acquisition of up to 50 MS/MS spectra over 2.5 s, for a total cycle time of 2.8 s.

The MS/MS spectra were analyzed using ProteinPilot 5.0.1 software based on the Paragon Algorithm Build 5.0.1.0.4874 contained in the software. The spectra were searched against the Arabidopsis database on the NCBI website (http://www.ncbi.nlm.nih.gov/protein) plus 536 common human and laboratory contaminants (ABSciex_ContaminantDB_20070711).

Western-Blot Assays

The cytosolic, plasma membrane, and microsome fractions of proteins extracted as described above were separated on a 10% SDS-PAGE gel and transferred to a nitrocellulose membrane (GE Healthcare) in Tris-Gly buffer. Membranes were blocked in PBST (PBS + 0.05% Tween 20) with 5% nonfat milk for 1 h at room temperature and incubated in the presence of anti-FLAG primary antibody (Clontech) for FLAG-AGB1 or anti-AHA primary antibody (Hayashi et al., 2010) for AHA overnight at 4°C. The membranes were washed three times in PBST for 10 min each, then incubated with a goat anti-mouse IgG conjugated to horseradish peroxidase (Promega) for FLAG-AGB1 and a goat anti-rabbit IgG conjugated to horseradish peroxidase (Promega) for AHA for 1 h at room temperature, then washed again three times in PBST for 10 min each and twice in PBS for 5 min each. Chemiluminescence signals were generated by applying SuperSignal West Dura Extended Duration Substrate (ThermoFisher) to the membrane and visualized using the Gel Logic 4000 Pro imaging system (Carestream).

BiFC Assays

BiFC assays were performed using an improved BiFC system in *Nicotiana benthamiana* (Gookin and Assmann, 2014). Initially, a 2,685-bp full-length cDNA of *FER* (At3G51550) was inserted into MCS1 of the pDOE-9 and pDOE-10 BiFC vectors using restriction sites *Nco*I and *Spe*I and the In-Fusion Cloning Kit (Clontech) to create Ubiquitin10 promoter-driven *FER:NVen210* parent vectors. However, expressing full-length FER in parent vectors caused cell death and autofluorescence. Therefore, following previous publications, the C-terminal kinase domain of *FER* (*FERCT*; amino acids 469–895) and a kinase-inactive version of *FER* (*FERK565R*) were inserted to create parent vectors

(Escobar-Restrepo et al., 2007; Haruta et al., 2014; Shih et al., 2014) using the same process. *GPA1*, *XLG1*, *XLG2*, and *XLG3* cDNA were inserted into MCS3 of the pDOE-09 parent vector using *San*DI and *Aat*II restriction sties to create *FERCT/FERK565R:NVen210-GPA1/XLG1/XLG2/XLG3:CVen210* BiFC constructs, and *AGB1* was inserted into MCS3 of the pDOE-10 parent vector to create *FERCT/FERK565R:NVen210-CVen210:AGB1* constructs. The constructs of *NVen210:AGB1-OST1/ABI1/ABI2:CVen210* were made using the same strategy.

We previously showed that AGGs facilitate the interaction between AGB1 and Gαs (GPA1, XLG1, XLG2, and XLG3) in BiFC (Gookin and Assmann, 2014; Chakravorty et al., 2015). Here, an untagged, 35S promoter-driven *AGG1AGG2* construct was made by removing mTurquoise and inserting *AGG1* cDNA into MCS1 of the pDOE-14 vector using *Nco*I and *Xba*I restriction enzymes and removing mVenus and inserting *AGG2* cDNA into MCS3 using *San*DI and *Asi*SI restriction enzyme sites. Alternatively, *AGG1*, *AGG2*, or *AGG3* cDNA was inserted into pDOE-14 vector using *Nco*I and *Asi*SI sites to create untagged *AGG1*, *AGG2*, or *AGG3*. A final infiltration OD$_{600}$ of 0.008 or 0.02 was used to reduce the false-positive results that can arise from overexpression (Gookin and Assmann, 2014). Constructs for direct comparison were infiltrated on the same leaves, and two plants with two leaves on each plant were used for each replicate. At least two replicates were performed for each experimental sample. Images were taken using a 40× objective at ~48 h and ~60 h after infiltration. For BiFC quantification, relative fluorescence intensity in the mVenus channel was calculated after adjusting the threshold to subtract the background signals in the vacuole and residual autofluorescence in the chloroplast using ImageJ. The averages of relative fluorescence intensities were calculated using three to 11 images in the parent vector control and five to 13 images in each experimental sample (Kudla and Bock, 2016).

Stomatal Aperture Experiments

For experiments assaying stomatal opening, intact leaves of 4- to 5-week-old plants grown in soil were excised into ~4- × 8-mm^2 pieces and incubated in a clear 24-well Falcon polystyrene microplate in 500 μL of 10 mM KCl, 7.5 mM iminodiacetic acid, and 10 mM MES-KOH, pH 6.15, in the dark for 2 h to initially close stomata. Figure 2A and Supplemental Figure S5 provide initial apertures for Col and *fer-4*, showing that our pretreatment effectively results in a baseline of closed stomata prior to exposure to white light as a stimulus for stomatal opening. We verified this closed baseline, with apertures similar to those provided in Figure 2A and Supplemental Figure S5, in all experiments that assayed stomatal opening. Then, leaf pieces were treated with or without 1 or 10 μM synthesized active form of RALF1 (amino acids 72–120 of the precursor; Biomatik) or RALF1Δ (which lacks amino acids 2–8 of the active form/amino acids 73–79 of the precursor; Biomatik) in the light (light intensity ~150 μmol m^{-2} s^{-1}) for another 3 h. For experiments assaying stomatal closure, intact leaves were excised and incubated in 500 μL of 20 mM KCl, 0.5 mM CaCl$_2$, and 5 mM MES-KOH, pH 6.15, for 3 h in the light to initially open stomata, then treated with or without 1 or 10 μM synthesized active form of RALF1, or inactive RALF1Δ, for another 2 h in the light. Images of stomatal apertures were taken and measured as described previously (Yu and Assmann, 2015). Three to four independent blinded experiments were performed for each assay.

RT-PCR and Real-Time qRT-PCR

Total RNA was isolated from rosette leaves, 2-week-old whole seedlings, siliques, or highly purified guard cell protoplasts (Zhu et al., 2016) using the NucleoSpin RNA Plant kit (Macherey-Nagel) and treated with RQ1 RNase-Free DNase (Promega) to remove DNA contamination following the manufacturers' instructions. Two micrograms of RNA was reverse transcribed into cDNA using the SuperScript III Reverse Transcriptase kit (Invitrogen), and the cDNA was diluted three times for use as a template in qRT-PCR. qRT-PCR was performed using SYBR Green (Bio-Rad) to detect synthesized double-stranded DNA in the IQ5 Multicolor Real-Time PCR Detection System (Bio-Rad). The cycling conditions comprised a 5-min denaturation at 95°C, 40 cycles at 95°C for 30 s, 62°C for 30 s, and 72°C for 40 s, and a final extension cycle at 72°C for 8 min. Actin2/8 was used as the reference to normalize gene expression. Three independent biological experiments with three technical replicates each were performed. The gene-specific primers used in qRT-PCR and RT-PCR were as follows: Actin2/8 FP, 5'-GGTAACATTGTGCTCAGTGGTGG-3'; Actin2/8 RP, 5'-AACGACCTTAATCTTCATGCTGC-3'; XLG3 FP, 5'-ATGGAGAAGAAA-GATGAAGGTGAAAGC-3'; XLG3 RP, 5'-GCTCTAAGCACACAGTTTCCA-CAATACTT-3'; RALF1 FP, 5'-ACTCTTACGATTCTCGTCGT-3'; and RALF1 RP, 5'-TGCAACCACGACTATAAGGA-3'.

Supplemental Data

The following supplemental materials are available.

Supplemental Figure S1. Western blot showing that AGB1 is enriched in the plasma membrane fraction.

Supplemental Figure S2. BiFC quantification of the interactions between AGB1/AGGs and FER.

Supplemental Figure S3. FER does not interact with GPA1, XLG1, XLG2, or XLG3 in BiFC.

Supplemental Figure S4. *RALF1* expression in guard cells.

Supplemental Figure S5. The *fer-4* mutant is insensitive to RALF1 effects on stomatal movement.

Supplemental Figure S6. AGB1 may interact with ABI2 in the presence of AGG1/AGG2 but not in the presence of AGG3.

Supplemental Figure S7. RT-PCR for *xlg3* mutants.

Supplemental Table S1. Confidently identified proteins found in AGB1 co-IP but not in the Col control.

Supplemental Table S2. All of the proteins found in AGB1 co-IP but not in the Col control.

Supplemental Table S3. Peptides of the proteins shown in Table I.

Supplemental Table S4. All of the proteins identified in the Col control.

LITERATURE CITED

Acharya BR, Jeon BW, Zhang W, Assmann SM (2013) Open Stomata 1 (OST1) is limiting in abscisic acid responses of Arabidopsis guard cells. New Phytol **200:** 1049–1063

Alexandersson E, Gustavsson N, Bernfur K, Karlsson A, Kjellbom P, Larsson C (2008) Purification and proteomic analysis of plant plasma membranes. *In* D Pflieger, J Rossier, eds, Organelle Proteomics. Methods in Molecular Biology, Vol 432. Humana Press, Totowa, NJ, pp 161–173

Allen GJ, Chu SP, Harrington CL, Schumacher K, Hoffmann T, Tang YY, Grill E, Schroeder JI (2001) A defined range of guard cell calcium oscillation parameters encodes stomatal movements. Nature **411:** 1053–1057

Anderson DJ, Botella JR (2007) Expression analysis and subcellular localization of the Arabidopsis thaliana G-protein β-subunit AGB1. Plant Cell Rep **26:** 1469–1480

Aranda-Sicilia MN, Trusov Y, Maruta N, Chakravorty D, Zhang Y, Botella JR (2015) Heterotrimeric G proteins interact with defense-related receptor-like kinases in Arabidopsis. J Plant Physiol **188:** 44–48

Bellati J, Champeyroux C, Hem S, Rofidal V, Krouk G, Maurel C, Santoni V (2016) Novel aquaporin regulatory mechanisms revealed by interactomics. Mol Cell Proteomics **15:** 3473–3487

Bommert P, Je BI, Goldshmidt A, Jackson D (2013) The maize Gα gene COMPACT PLANT2 functions in CLAVATA signalling to control shoot meristem size. Nature **502:** 555–558

Botto JF, Ibarra S, Jones AM (2009) The heterotrimeric G-protein complex modulates light sensitivity in *Arabidopsis thaliana* seed germination. Photochem Photobiol **85:** 949–954

Brückner A, Polge C, Lentze N, Auerbach D, Schlattner U (2009) Yeast two-hybrid, a powerful tool for systems biology. Int J Mol Sci **10:** 2763–2788

Chakravorty D, Gookin TE, Milner MJ, Yu Y, Assmann SM (2015) Extra-large G proteins expand the repertoire of subunits in Arabidopsis heterotrimeric G protein signaling. Plant Physiol **169:** 512–529

Chakravorty D, Trusov Y, Zhang W, Acharya BR, Sheahan MB, McCurdy DW, Assmann SM, Botella JR (2011) An atypical heterotrimeric G-protein γ-subunit is involved in guard cell K⁺-channel regulation and morphological development in *Arabidopsis thaliana*. Plant J **67:** 840–851

Chen J, Yu F, Liu Y, Du C, Li X, Zhu S, Wang X, Lan W, Rodriguez PL, Liu X, et al (2016) FERONIA interacts with ABI2-type phosphatases to facilitate signaling cross-talk between abscisic acid and RALF peptide in Arabidopsis. Proc Natl Acad Sci USA **113:** E5519–E5527

Clough SJ, Bent AF (1998) Floral dip: a simplified method for Agrobacterium-mediated transformation of *Arabidopsis thaliana*. Plant J **16:** 735–743

Delgado-Cerezo M, Sánchez-Rodríguez C, Escudero V, Miedes E, Fernández PV, Jordá L, Hernández-Blanco C, Sánchez-Vallet A, Bednarek P, Schulze-Lefert P, et al (2012) Arabidopsis heterotrimeric G-protein regulates cell wall defense and resistance to necrotrophic fungi. Mol Plant **5:** 98–114

Deslauriers SD, Larsen PB (2010) FERONIA is a key modulator of brassinosteroid and ethylene responsiveness in Arabidopsis hypocotyls. Mol Plant **3:** 626–640

Ding L, Pandey S, Assmann SM (2008) Arabidopsis extra-large G proteins (XLGs) regulate root morphogenesis. Plant J **53:** 248–263

Duan Q, Kita D, Li C, Cheung AY, Wu HM (2010) FERONIA receptor-like kinase regulates RHO GTPase signaling of root hair development. Proc Natl Acad Sci USA **107:** 17821–17826

Earley KW, Haag JR, Pontes O, Opper K, Juehne T, Song K, Pikaard CS (2006) Gateway-compatible vectors for plant functional genomics and proteomics. Plant J **45:** 616–629

Escobar-Restrepo JM, Huck N, Kessler S, Gagliardini V, Gheysenlinck J, Yang WC, Grossniklaus U (2007) The FERONIA receptor-like kinase mediates male-female interactions during pollen tube reception. Science **317:** 656–660

Fan LM, Zhang W, Chen JG, Taylor JP, Jones AM, Assmann SM (2008) Abscisic acid regulation of guard-cell K⁺ and anion channels in Gβ- and RGS-deficient Arabidopsis lines. Proc Natl Acad Sci USA **105:** 8476–8481

Fan LM, Zhao Z, Assmann SM (2004) Guard cells: a dynamic signaling model. Curr Opin Plant Biol **7:** 537–546

Fredriksson R, Schiöth HB (2005) The repertoire of G-protein-coupled receptors in fully sequenced genomes. Mol Pharmacol **67:** 1414–1425

Galvez-Valdivieso G, Fryer MJ, Lawson T, Slattery K, Truman W, Smirnoff N, Asami T, Davies WJ, Jones AM, Baker NR, et al (2009) The high light response in *Arabidopsis* involves ABA signaling between vascular and bundle sheath cells. Plant Cell **21:** 2143–2162

Gookin TE, Assmann SM (2014) Significant reduction of BiFC non-specific assembly facilitates in planta assessment of heterotrimeric G-protein interactors. Plant J **80:** 553–567

Haruta M, Monshausen G, Gilroy S, Sussman MR (2008) A cytoplasmic Ca²⁺ functional assay for identifying and purifying endogenous cell signaling peptides in Arabidopsis seedlings: identification of AtRALF1 peptide. Biochemistry **47:** 6311–6321

Haruta M, Sabat G, Stecker K, Minkoff BB, Sussman MR (2014) A peptide hormone and its receptor protein kinase regulate plant cell expansion. Science **343:** 408–411

Hayashi M, Inoue S, Takahashi K, Kinoshita T (2011) Immunohistochemical detection of blue light-induced phosphorylation of the plasma membrane H⁺-ATPase in stomatal guard cells. Plant Cell Physiol **52:** 1238–1248

Hayashi Y, Nakamura S, Takemiya A, Takahashi Y, Shimazaki K, Kinoshita T (2010) Biochemical characterization of in vitro phosphorylation and dephosphorylation of the plasma membrane H⁺-ATPase. Plant Cell Physiol **51:** 1186–1196

Huang J, Taylor JP, Chen JG, Uhrig JF, Schnell DJ, Nakagawa T, Korth KL, Jones AM (2006) The plastid protein THYLAKOID FORMATION1 and the plasma membrane G-protein GPA1 interact in a novel sugar-signaling mechanism in *Arabidopsis*. Plant Cell **18:** 1226–1238

Hubbard KE, Nishimura N, Hitomi K, Getzoff ED, Schroeder JI (2010) Early abscisic acid signal transduction mechanisms: newly discovered components and newly emerging questions. Genes Dev **24:** 1695–1708

Ishida T, Tabata R, Yamada M, Aida M, Mitsumasu K, Fujiwara M, Yamaguchi K, Shigenobu S, Higuchi M, Tsuji H, et al (2014)

Heterotrimeric G proteins control stem cell proliferation through CLAVATA signaling in Arabidopsis. EMBO Rep **15:** 1202–1209

Jaiswal DK, Werth EG, McConnell EW, Hicks LM, Jones AM (2016) Time-dependent, glucose-regulated Arabidopsis Regulator of G-protein Signaling 1 network. Curr Plant Biol **5:** 25–35

Jin X, Wang RS, Zhu M, Jeon BW, Albert R, Chen S, Assmann SM (2013) Abscisic acid-responsive guard cell metabolomes of *Arabidopsis* wild-type and *gpa1* G-protein mutants. Plant Cell **25:** 4789–4811

Jones AM, Assmann SM (2004) Plants: the latest model system for G-protein research. EMBO Rep **5:** 572–578

Jones AM, Ecker JR, Chen JG (2003) A reevaluation of the role of the heterotrimeric G protein in coupling light responses in Arabidopsis. Plant Physiol **131:** 1623–1627

Jones AM, Xuan Y, Xu M, Wang RS, Ho CH, Lalonde S, You CH, Sardi MI, Parsa SA, Smith-Valle E, et al (2014) Border control: a membrane-linked interactome of Arabidopsis. Science **344:** 711–716

Joo JH, Wang S, Chen JG, Jones AM, Fedoroff NV (2005) Different signaling and cell death roles of heterotrimeric G protein α and β subunits in the Arabidopsis oxidative stress response to ozone. Plant Cell **17:** 957–970

Joshi-Saha A, Valon C, Leung J (2011) Abscisic acid signal off the STARting block. Mol Plant **4:** 562–580

Kansup J, Tsugama D, Liu S, Takano T (2013) The Arabidopsis adaptor protein AP-3μ interacts with the G-protein β subunit AGB1 and is involved in abscisic acid regulation of germination and post-germination development. J Exp Bot **64:** 5611–5621

Kansup J, Tsugama D, Liu S, Takano T (2014) Arabidopsis G-protein β subunit AGB1 interacts with NPH3 and is involved in phototropism. Biochem Biophys Res Commun **445:** 54–57

Keinath NF, Kierszniowska S, Lorek J, Bourdais G, Kessler SA, Shimosato-Asano H, Grossniklaus U, Schulze WX, Robatzek S, Panstruga R (2010) PAMP (pathogen-associated molecular pattern)-induced changes in plasma membrane compartmentalization reveal novel components of plant immunity. J Biol Chem **285:** 39140–39149

Kinoshita T, Shimazaki Ki (1999) Blue light activates the plasma membrane H$^+$-ATPase by phosphorylation of the C-terminus in stomatal guard cells. EMBO J **18:** 5548–5558

Klopffleisch K, Phan N, Augustin K, Bayne RS, Booker KS, Botella JR, Carpita NC, Carr T, Chen JG, Cooke TR, et al (2011) Arabidopsis G-protein interactome reveals connections to cell wall carbohydrates and morphogenesis. Mol Syst Biol **7:** 532

Kobayashi S, Tsugama D, Liu S, Takano T (2012) A U-box E3 ubiquitin ligase, PUB20, interacts with the Arabidopsis G-protein β subunit, AGB1. PLoS ONE **7:** e49207

Kudla J, Bock R (2016) Lighting the way to protein-protein interactions: recommendations on best practices for bimolecular fluorescence complementation analyses. Plant Cell **28:** 1002–1008

Kwak JM, Mori IC, Pei ZM, Leonhardt N, Torres MA, Dangl JL, Bloom RE, Bodde S, Jones JD, Schroeder JI (2003) NADPH oxidase AtrbohD and AtrbohF genes function in ROS-dependent ABA signaling in Arabidopsis. EMBO J **22:** 2623–2633

Lapik YR, Kaufman LS (2003) The *Arabidopsis* cupin domain protein At-Pirin1 interacts with the G protein α-subunit GPA1 and regulates seed germination and early seedling development. Plant Cell **15:** 1578–1590

Lee YR, Assmann SM (1999) *Arabidopsis thaliana* 'extra-large GTP-binding protein' (AtXLG1): a new class of G-protein. Plant Mol Biol **40:** 55–64

Li C, Yeh FL, Cheung AY, Duan Q, Kita D, Liu MC, Maman J, Luu EJ, Wu BW, Gates L, et al (2015) Glycosylphosphatidylinositol-anchored proteins as chaperones and co-receptors for FERONIA receptor kinase signaling in Arabidopsis. eLife **4:** e06587

Li FC, Wang J, Wu MM, Fan CM, Li X, He JM (2017) Mitogen-activated protein kinase phosphatases affect UV-B-induced stomatal closure via controlling NO in guard cells. Plant Physiol **173:** 760–770

Liang X, Ding P, Lian K, Wang J, Ma M, Li L, Li L, Li M, Zhang X, Chen S, et al (2016) Arabidopsis heterotrimeric G proteins regulate immunity by directly coupling to the FLS2 receptor. eLife **5:** e13568

Lindner H, Müller LM, Boisson-Dernier A, Grossniklaus U (2012) CrRLK1L receptor-like kinases: not just another brick in the wall. Curr Opin Plant Biol **15:** 659–669

Liu J, Ding P, Sun T, Nitta Y, Dong O, Huang X, Yang W, Li X, Botella JR, Zhang Y (2013) Heterotrimeric G proteins serve as a converging point in plant defense signaling activated by multiple receptor-like kinases. Plant Physiol **161:** 2146–2158

Llorente F, Alonso-Blanco C, Sánchez-Rodriguez C, Jorda L, Molina A (2005) ERECTA receptor-like kinase and heterotrimeric G protein from Arabidopsis are required for resistance to the necrotrophic fungus *Plectosphaerella cucumerina*. Plant J **43:** 165–180

Lorek J, Griebel T, Jones AM, Kuhn H, Panstruga R (2013) The role of Arabidopsis heterotrimeric G-protein subunits in MLO2 function and MAMP-triggered immunity. Mol Plant Microbe Interact **26:** 991–1003

Ma H, Yanofsky MF, Meyerowitz EM (1990) Molecular cloning and characterization of GPA1, a G protein α subunit gene from *Arabidopsis thaliana*. Proc Natl Acad Sci USA **87:** 3821–3825

Maruta N, Trusov Y, Brenya E, Parekh U, Botella JR (2015) Membrane-localized extra-large G proteins and G$\beta\gamma$ of the heterotrimeric G proteins form functional complexes engaged in plant immunity in Arabidopsis. Plant Physiol **167:** 1004–1016

Mason MG, Botella JR (2000) Completing the heterotrimer: isolation and characterization of an *Arabidopsis thaliana* G protein γ-subunit cDNA. Proc Natl Acad Sci USA **97:** 14784–14788

Mason MG, Botella JR (2001) Isolation of a novel G-protein γ-subunit from *Arabidopsis thaliana* and its interaction with Gβ. Biochim Biophys Acta **1520:** 147–153

Montillet JL, Leonhardt N, Mondy S, Tranchimand S, Rumeau D, Boudsocq M, Garcia AV, Douki T, Bigeard J, Laurière C, et al (2013) An abscisic acid-independent oxylipin pathway controls stomatal closure and immune defense in Arabidopsis. PLoS Biol **11:** e1001513

Mudgil Y, Uhrig JF, Zhou J, Temple B, Jiang K, Jones AM (2009) *Arabidopsis* N-MYC DOWNREGULATED-LIKE1, a positive regulator of auxin transport in a G protein-mediated pathway. Plant Cell **21:** 3591–3609

Murphy E, De Smet I (2014) Understanding the RALF family: a tale of many species. Trends Plant Sci **19:** 664–671

Mustilli AC, Merlot S, Vavasseur A, Fenzi F, Giraudat J (2002) *Arabidopsis* OST1 protein kinase mediates the regulation of stomatal aperture by abscisic acid and acts upstream of reactive oxygen species production. Plant Cell **14:** 3089–3099

Obrdlik P, Neuhaus G, Merkle T (2000) Plant heterotrimeric G protein β subunit is associated with membranes via protein interactions involving coiled-coil formation. FEBS Lett **476:** 208–212

Olsson A, Svennelid F, Ek B, Sommarin M, Larsson C (1998) A phosphothreonine residue at the C-terminal end of the plasma membrane H$^+$-ATPase is protected by fusicoccin-induced 14-3-3 binding. Plant Physiol **118:** 551–555

Pandey S, Assmann SM (2004) The *Arabidopsis* putative G protein-coupled receptor GCR1 interacts with the G protein α subunit GPA1 and regulates abscisic acid signaling. Plant Cell **16:** 1616–1632

Pandey S, Chen JG, Jones AM, Assmann SM (2006) G-protein complex mutants are hypersensitive to abscisic acid regulation of germination and postgermination development. Plant Physiol **141:** 243–256

Pandey S, Wang RS, Wilson L, Li S, Zhao Z, Gookin TE, Assmann SM, Albert R (2010) Boolean modeling of transcriptome data reveals novel modes of heterotrimeric G-protein action. Mol Syst Biol **6:** 372

Pearce G, Moura DS, Stratmann J, Ryan CA Jr (2001) RALF, a 5-kDa ubiquitous polypeptide in plants, arrests root growth and development. Proc Natl Acad Sci USA **98:** 12843–12847

Pei Z-M, Murata Y, Benning G, Thomine S, Klüsener B, Allen GJ, Grill E, Schroeder JI (2000) Calcium channels activated by hydrogen peroxide mediate abscisic acid signalling in guard cells. Nature **406:** 731–734

Perfus-Barbeoch L, Jones AM, Assmann SM (2004) Plant heterotrimeric G protein function: insights from Arabidopsis and rice mutants. Curr Opin Plant Biol **7:** 719–731

Qiu QS, Guo Y, Dietrich MA, Schumaker KS, Zhu JK (2002) Regulation of SOS1, a plasma membrane Na$^+$/H$^+$ exchanger in *Arabidopsis thaliana*, by SOS2 and SOS3. Proc Natl Acad Sci USA **99:** 8436–8441

Sato A, Sato Y, Fukao Y, Fujiwara M, Umezawa T, Shinozaki K, Hibi T, Taniguchi M, Miyake H, Goto DB, et al (2009) Threonine at position 306 of the KAT1 potassium channel is essential for channel activity and is a target site for ABA-activated SnRK2/OST1/SnRK2.6 protein kinase. Biochem J **424:** 439–448

Shih HW, Miller ND, Dai C, Spalding EP, Monshausen GB (2014) The receptor-like kinase FERONIA is required for mechanical signal transduction in Arabidopsis seedlings. Curr Biol **24:** 1887–1892

Stegmann M, Monaghan J, Smakowska-Luzan E, Rovenich H, Lehner A, Holton N, Belkhadir Y, Zipfel C (2017) The receptor kinase FER is a

RALF-regulated scaffold controlling plant immune signaling. Science **355**: 287–289

Taddese B, Upton GJ, Bailey GR, Jordan SR, Abdulla NY, Reeves PJ, Reynolds CA (2014) Do plants contain G protein-coupled receptors? Plant Physiol **164**: 287–307

Thung L, Trusov Y, Chakravorty D, Botella JR (2012) Gγ1+Gγ2+Gγ3=Gβ: the search for heterotrimeric G-protein γ subunits in Arabidopsis is over. J Plant Physiol **169**: 542–545

Trinkle-Mulcahy L, Boulon S, Lam YW, Urcia R, Boisvert FM, Vandermoere F, Morrice NA, Swift S, Rothbauer U, Leonhardt H, et al (2008) Identifying specific protein interaction partners using quantitative mass spectrometry and bead proteomes. J Cell Biol **183**: 223–239

Trusov Y, Botella JR (2016) Plant G-proteins come of age: breaking the bond with animal models. Front Chem **4**: 24

Trusov Y, Rookes JE, Chakravorty D, Armour D, Schenk PM, Botella JR (2006) Heterotrimeric G proteins facilitate Arabidopsis resistance to necrotrophic pathogens and are involved in jasmonate signaling. Plant Physiol **140**: 210–220

Tsugama D, Liu H, Liu S, Takano T (2012) Arabidopsis heterotrimeric G protein β subunit interacts with a plasma membrane 2C-type protein phosphatase, PP2C52. Biochim Biophys Acta **1823**: 2254–2260

Tsugama D, Liu S, Takano T (2013) A bZIP protein, VIP1, interacts with Arabidopsis heterotrimeric G protein β subunit, AGB1. Plant Physiol Biochem **71**: 240–246

Ullah H, Chen JG, Temple B, Boyes DC, Alonso JM, Davis KR, Ecker JR, Jones AM (2003) The β-subunit of the *Arabidopsis* G protein negatively regulates auxin-induced cell division and affects multiple developmental processes. Plant Cell **15**: 393–409

Ullah H, Chen JG, Wang S, Jones AM (2002) Role of a heterotrimeric G protein in regulation of Arabidopsis seed germination. Plant Physiol **129**: 897–907

Ullah H, Chen JG, Young JC, Im KH, Sussman MR, Jones AM (2001) Modulation of cell proliferation by heterotrimeric G protein in Arabidopsis. Science **292**: 2066–2069

Urano D, Maruta N, Trusov Y, Stoian R, Wu Q, Liang Y, Jaiswal DK, Thung L, Jackson D, Botella JR, et al (2016a) Saltational evolution of the heterotrimeric G protein signaling mechanisms in the plant kingdom. Sci Signal **9**: ra93

Urano D, Miura K, Wu Q, Iwasaki Y, Jackson D, Jones AM (2016b) Plant morphology of heterotrimeric G protein mutants. Plant Cell Physiol **57**: 437–445

Wang XQ, Ullah H, Jones AM, Assmann SM (2001) G protein regulation of ion channels and abscisic acid signaling in Arabidopsis guard cells. Science **292**: 2070–2072

Wang Y, Wu Y, Yu B, Yin Z, Xia Y (2017) Extra-large G proteins interact with E3 ligases PUB4 and PUB2 and function in cytokinin and developmental processes. Plant Physiol **173**: 1235–1246

Warpeha KM, Lateef SS, Lapik Y, Anderson M, Lee BS, Kaufman LS (2006) G-protein-coupled receptor 1, G-protein Gα-subunit 1, and prephenate dehydratase 1 are required for blue light-induced production of phenylalanine in etiolated Arabidopsis. Plant Physiol **140**: 844–855

Weiss CA, Garnaat CW, Mukai K, Hu Y, Ma H (1994) Isolation of cDNAs encoding guanine nucleotide-binding protein β-subunit homologs from maize (ZGB1) and *Arabidopsis* (AGB1). Proc Natl Acad Sci USA **91**: 9554–9558

Xing S, Wallmeroth N, Berendzen KW, Grefen C (2016) Techniques for the analysis of protein-protein interactions in vivo. Plant Physiol **171**: 727–758

Xu DB, Chen M, Ma YN, Xu ZS, Li LC, Chen YF, Ma YZ (2015) A G-protein β subunit, AGB1, negatively regulates the ABA response and drought tolerance by down-regulating AtMPK6-related pathway in Arabidopsis. PLoS ONE **10**: e0116385

Yu F, Qian L, Nibau C, Duan Q, Kita D, Levasseur K, Li X, Lu C, Li H, Hou C, et al (2012) FERONIA receptor kinase pathway suppresses abscisic acid signaling in Arabidopsis by activating ABI2 phosphatase. Proc Natl Acad Sci USA **109**: 14693–14698

Yu TY, Shi DQ, Jia PF, Tang J, Li HJ, Liu J, Yang WC (2016) The Arabidopsis receptor kinase ZAR1 is required for zygote asymmetric division and its daughter cell fate. PLoS Genet **12**: e1005933

Yu Y, Assmann SM (2015) The heterotrimeric G-protein β subunit, AGB1, plays multiple roles in the Arabidopsis salinity response. Plant Cell Environ **38**: 2143–2156

Zhu H, Li GJ, Ding L, Cui X, Berg H, Assmann SM, Xia Y (2009) Arabidopsis extra large G-protein 2 (XLG2) interacts with the Gβ subunit of heterotrimeric G protein and functions in disease resistance. Mol Plant **2**: 513–525

Zhu M, Jeon BW, Geng S, Yu Y, Balmant K, Chen S, Assmann SM (2016) Preparation of epidermal peels and guard cell protoplasts for cellular, electrophysiological, and -omics assays of guard cell function. Methods Mol Biol **1363**: 89–121